

Highly ordered anodic alumina nanotemplate with about 14 nm diameter

Tae-Yong Kim and Soo-Hwan Jeong[†]

Department of Chemical Engineering, Kyungpook National University, Daegu 702-701, Korea

(Received 29 January 2008 • accepted 21 February 2008)

Abstract—A novel method for the fabrication of highly ordered nanopore arrays with very small diameter of 14 nm was demonstrated by using low-temperature anodization. Two-step anodization was carried out at 25 V, sulfuric acid concentration of 0.3 M, and electrolyte temperature of -15 °C. After anodization, a regular pore array with mean diameter of 14 nm and interpore distance of 65 nm was formed. The pore diameter and regular arrangement were confirmed by scanning electron microscopy (SEM) and fast Fourier transformation (FFT), respectively. The present results strongly suggest that the diameter of pores in a highly ordered alumina template can be reduced by lowering the anodization temperature.

Key words: Porous Alumina, Anodization, Pore Diameter, Pore Arrangement

INTRODUCTION

There have been increasing concerns that there are not only technological but also economical limitations in currently used lithographic technologies based on optical, electron or X-ray beams for next-generation device fabrication [1,2]. For this reason, much attention has been paid to nanostructure formation by self-organizing methods such as nanopore formation by Al anodization [3], strain-induced nanostructure formation [4], and nanowire formation on the atomic step edges [5]. Among these methods, the increasing attraction to nanopore formation by Al anodization is mainly due to its relatively easy and cost-effective processing, and its capability of realizing extremely highly ordered cylindrical pore arrays with high density ($\sim 10^{10}/\text{cm}^2$). By using the pore arrays as a template for nanomaterial synthesis, these features facilitate the growth of ordered arrays of multiwalled carbon nanotubes, and even the manufacture of ultrahigh-density magnetic recording materials, nanowires of other metals and semiconductors. When the bottom of the pores is opened, the resulting nanoholes can be used for gas-separating membranes [6], particle-sieving filters [7], and as a pattern-transfer nanomask [8]. The ordered pore arrays can also be used as a two-dimensional (2D) photonic crystal [9].

Currently, however, highly ordered pore arrays can be fabricated only at a specific voltage that is dependent on the acid species. The most commonly used electrolytes for the preparation of porous alumina are sulfuric acid, oxalic acid, and phosphoric acid, depending on the pore diameter and pore density required. To date, it is possible to fabricate well defined and highly ordered porous alumina with diameter larger than 20 nm by using sulfuric acid as anodization electrolyte. Recently, Nielsch et al. reported the highly ordered porous alumina with 24 nm diameter by using sulfuric acid as anodization electrolyte [10]. However, some applications often need smaller diameters. For example, room temperature quantum devices, such as ballistic transistor and interconnector and devices utilizing single electron phenomena, requires smaller pattern size [11]. Xu et

al. [12] proposed a grazing ion milling of the U-shaped barrier layer in porous alumina in order to obtain nanopore arrays with smaller diameter. However, this technique is too costly and time consuming. Moreover, one cannot obtain nanopore arrays with smaller diameter over the whole length of pores in this case because the preparation of smaller pore diameter at only the pore mouth region is possible.

In this paper, we report a novel method for the preparation of highly ordered porous alumina template with about 14 nm diameters by using a low temperature anodizing method.

EXPERIMENTAL

1. Preparation of Smooth Al Surface by Electropolishing

Prior to anodization, all of the high purity (99.999%) aluminum sheets were degreased in acetone with ultrasound and electropolished individually to remove large surface irregularities. Electropolishing was carried out by making specimen anodic in mixture solution of perchloric acid and ethanol ($\text{HClO}_4 : \text{C}_2\text{H}_5\text{OH} = 1 : 4$ in volumetric ration) for 2 min. The solution temperature was kept to be 7 °C with vigorous stirring. After electropolishing, samples were rinsed in an ethanol solution and dried. The mean roughness of the polished surface was measured by atomic force microscopy.

2. Anodization of Al Sheet

A two-step anodization was chosen to prepare an ordered porous alumina nanotemplate [3]. An Al sheet was anodized at 25 V in 0.3 M sulfuric acid solution at -15 °C for 12 hours. To induce a depression of the freezing point of electrolyte, ethylene glycol was chosen as inert additive during the anodizing process and added to the solution with a concentration of 5.4 M. After the anodic alumina film was chemically etched in a mixture of phosphoric acid and chromic acid solution, re-anodization was performed under the same conditions for 1 hour.

For some samples, pore diameters of alumina templates were enlarged by pore widening process in 5 wt% phosphoric acid in order to facilitate analysis of fast Fourier transformation (FFT). A schematic of the anodizing experiment is shown in Fig. 1.

3. Characterization of Samples

[†]To whom correspondence should be addressed.

E-mail: shjeong@knu.ac.kr

The morphology and the structure of AAO were observed with a field emission SEM (FE-SEM, Hitachi S-4300). We also ana-

lyzed SEM images of pores in alumina template by FFT to check the regularity of the pore arrangement.

RESULTS AND DISCUSSION

While the surface roughness of the aluminum sheet was in the range of several μm before electropolishing, the roughness of the electropolished samples was typically between 3 and 5 nm on a lateral length scale of 3 μm . To obtain hexagonally ordered pore array in porous alumina template, electropolishing is considered as an essential step.

Fig. 2 shows the SEM image of the alumina template after two-step anodization. The top view (inset in right upper corner) and cross-sectional views in inset of Fig. 2(a) and Fig. 2(a) demonstrate the high-aspect ratio appearance of ordered pore arrays in the anodic alumina template. From this image, the formation of straight parallel pores perpendicular to the substrate could be confirmed. Inter-pore distance of about 65 nm was also measured. Fig. 2(b) is a histogram of the measured pore diameter of porous alumina template. It is confirmed that the mean diameter and density of pores are 14.3 nm with narrow size distribution and 2.7×10^{10} pores/ cm^2 , respectively. To investigate the temperature dependence on pore diameter, we had carried out anodization at different temperatures (0 and 10 °C). The average of measured diameters of samples anodized at 0 and 10 °C was 16.5 and 18.6 nm, respectively. Based on three different anodizing experiments, the plot of $\ln(\text{pore diameter})$ versus $1/T$ shows good linearity. Therefore, we can conclude that pore formation is in good agreement with the Arrhenius law of reaction. It is also expected that further depression of anodizing temperature below -15 °C would produce even smaller pores.

In Fig. 3, steady-state pore growth of porous alumina is depicted. In general, steady-state pore growth in porous alumina during anodization process is explained as follows. Pores grow in vertical direction to the surface with an equilibrium of field-enhanced oxide chemical-dissolution at the acid solution/alumina interface and alumina formation at the alumina/aluminum interface [13]. Alumina formation results from the migration of oxygen-containing ions, such as O^{2-} and OH^- , from the anodizing solution across the alumina layer at the pore bottom. Meanwhile, some Al^{3+} ions under the electric field simultaneously move from aluminum metal to solution/alumina interface and are dissolved into the solution without contrib-

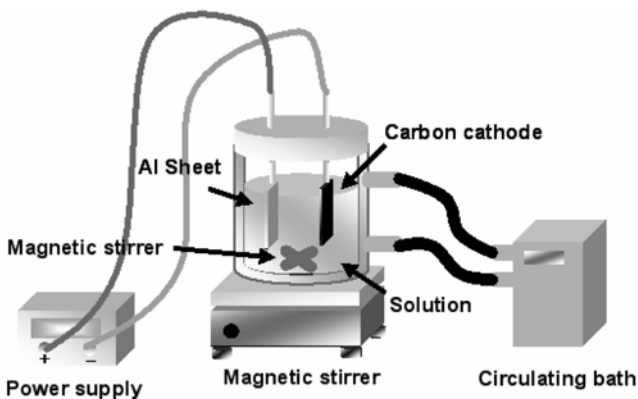


Fig. 1. Schematic of low-temperature aluminum anodizing apparatus.

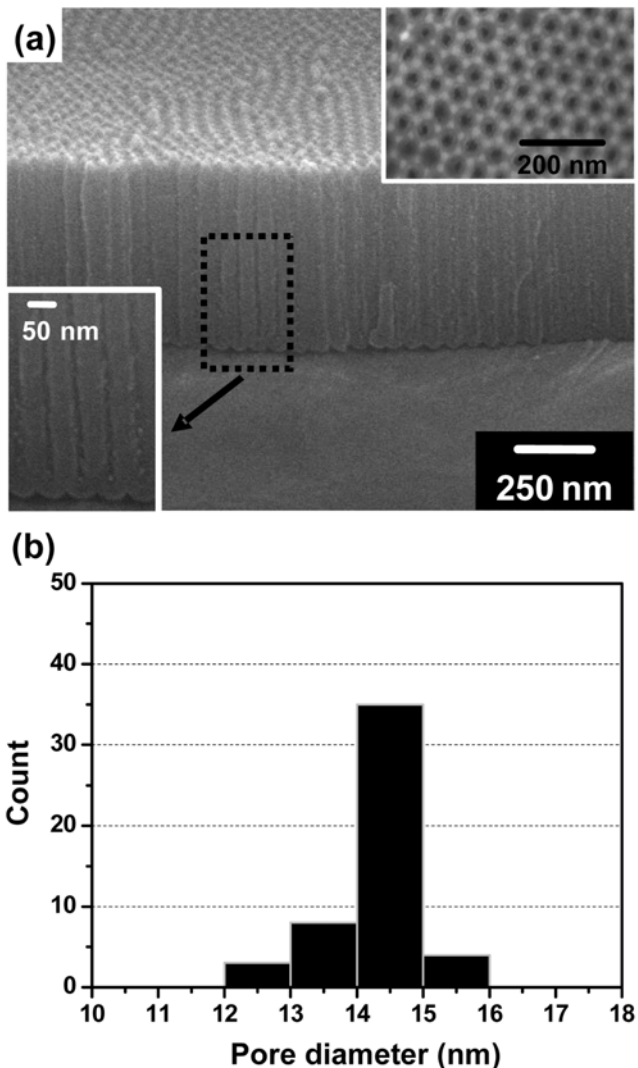


Fig. 2. (a) SEM image of ordered template. The insets are enlarged top and side view. (b) Histogram of measured pore diameter of porous alumina nanotemplate.

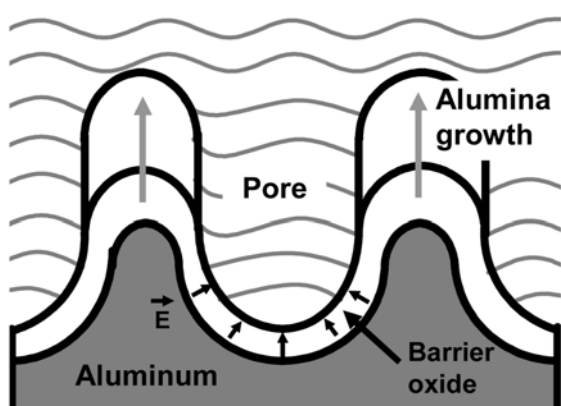


Fig. 3. Schematic of the pore growth of porous alumina.

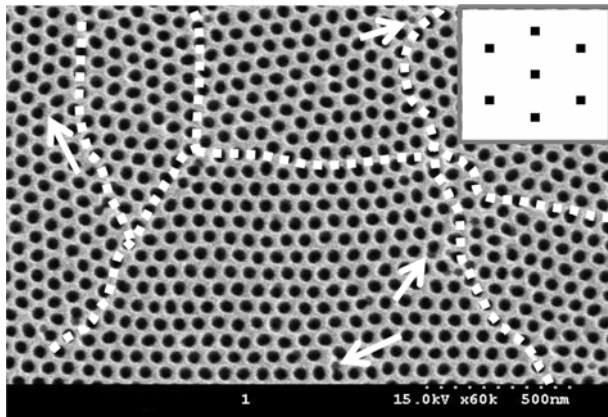


Fig. 4. SEM image of the top view of porous alumina template after pore widening by chemical etching [5 wt% phosphoric acid, 30 °C, 15 min]. The small arrows indicate point defects. Grain boundaries (as depicted with dotted lines) can also be seen. The inset is a result of FFT analysis.

uting to the alumina formation [14]. Under these steady-state conditions, a U-shaped interface propagates, resulting in straight pore growth in the upward direction [15]. In this context, suppression of anodizing temperature would lower the rate of field-assisted Al³⁺ dissolution into the solution. As a result, thicker pore wall formation and smaller diameter pore growth occurs under the low-temperature anodizing conditions.

In the case of a well-defined and highly-ordered porous alumina, the porosity (P) of a hexagonal structure can be defined by

$$P = \frac{\pi}{2\sqrt{3}} \left(\frac{D_{pore}}{D_{inter}} \right)^2 \quad (1)$$

D_{pore} and D_{inter} are pore diameter and interpore spacing in porous alumina template, respectively. Nielsch et al. [10] reported that self-ordering requires a porosity of 10%, independent of the specific anodizing electrolyte at normal temperatures. However, the estimated porosity of our samples by the above equation is 4.4%. It might be attributed to the depression of dissolution rate of Al³⁺ ions into the solution, resulting in small pore diameter.

To facilitate the observation of pore arrangement in porous alumina, the pore widening process was performed. From the resulting SEM image, we can observe an ordered pore arrangement with poly-domain characteristics, similar to 2D polycrystalline structure. The size of ordered domains is in the range of 500 nm-1 μm. Line defects at domain boundaries and a few point defects within the ordered domain are also observed. Within domain boundaries, the FFT pattern of the SEM image, as shown in inset of Fig. 4, exhibits a clear and obvious six-fold symmetry, confirming a single-crystalline pore arrangement. It is worthy of notice that our method can be applied to large area because anodization after indenting the Al surface with a concave mold enables us to prepare highly ordered porous alumina over a large area [16].

CONCLUSIONS

In conclusion, a novel method for the fabrication of highly or-

dered nanopore arrays with very small diameter of 14 nm was demonstrated by using low-temperature anodization. Two-step anodization was carried out at 25 V, sulfuric acid concentration of 0.3 M, and electrolyte temperature of -15 °C. After anodization, a regular pore array with mean diameter of 14 nm and interpore distance of 65 nm was formed. The present results suggest that the diameter of pores in a highly-ordered alumina template can be reduced by lowering the anodization temperature. We also expect that the method proposed in this letter would be very useful to the preparation of various nanomaterials by a template-based approach and many applications to nanomaterial-based devices.

ACKNOWLEDGMENT

This research was supported by Kyungpook National University Research Fund, 2005.

NOMENCLATURE

- P : porosity of alumina [%]
- D_{pore} : diameter of pore [nm]
- D_{inter} : interpore distance [nm]

REFERENCES

1. M. A. McCord, *J. Vac. Sci. Technol. B*, **15**, 2125 (1997).
2. J. J. Canning, *J. Vac. Sci. Technol. B*, **15**, 2109 (1997).
3. S.-K. Hwang, S.-H. Jeong, H.-Y. Hwang, O.-J. Lee and K.-H. Lee, *Korean J. Chem. Eng.*, **19**, 467 (2002).
4. R. Notzel, J. Temmyo and T. Tamamura, *Nature*, **369**, 131 (1994).
5. M. P. Zach, K. Ng and R. M. Penner, *Science*, **290**, 2120 (2000).
6. T. Kyotani, W. Xua, Y. Yokoyama, J. Inahara, H. Touhara and A. Tomita, *J. Membr. Sci.*, **196**, 231 (2002).
7. F. Li, J. He, W. L. Zhou and J. B. Wiley, *J. Am. Chem. Soc.*, **125**, 16166 (2003).
8. S.-H. Jeong, Y. K. Cha, I. K. Yoo, Y. S. Song and C. W. Chung, *Chem. Mater.*, **16**, 1612 (2004).
9. H. Masuda, M. Ohya, H. Asoh, M. Nakao, M. Nohtomi and T. Tamamura, *Jpn. J. Appl. Phys.*, **38**, L1403 (1999).
10. K. Nielss, J. Choi, K. Schwinn, R. B. Wehrspohn and U. Gösele, *Nano Lett.*, **2**, 677 (2002).
11. T. Xu, G. Zangari and R. M. Metzger, *Nano Lett.*, **2**, 37 (2002).
12. S. Shingubara, O. Okino, Y. Sayama, H. Sakaue and T. Takahagi, *Jpn. J. Appl. Phys.*, **36**, 7791 (1997).
13. V. P. Parkhutik and V. I. Shershulsky, *J. Phys. D: Appl. Phys.*, **25**, 1258 (1992).
14. O. Jessensky, F. Müller and U. Gösele, *Appl. Phys. Lett.*, **72**, 1173 (1998).
15. L. Zhang, H. S. Cho, F. Li, R. M. Metzger and W. D. Doyle, *J. Mater. Sci. Lett.*, **17**, 291 (1998).
16. H. Masuda, H. Yamada, M. Satoh, H. Asoh, M. Nakao and T. Tamamura, *Appl. Phys. Lett.*, **71**, 2770 (1997).